Peer-reviewed version available at Electronics 2018, 7, 79; doi:10.3390/electronics7060079

Article

A Performance Study of Massive MIMO Heterogeneous Networks with Ricean/Rayleigh Fading

James Kweku Nkrumah Nyarko *and Christian Ango Mbom

School of Electronics and Information Engineering, Northwestern Polytechnical University, Xi'an 710129, China; jnyarko@mail.nwpu.edu.cn and christianso2002@yahoo.com

* Correspondence: kwekujames80@yahoo.com

Abstract: The unprecedented demand for services and applications, coupled with large network architecture calls for a radical melioration in evolving wireless networks. Massive multiple-input and multiple-out (massive MIMO) systems, small cell networks (SCN) and Heterogeneous networks (HetNet) are envisioned to meet the new quality of service (QoS) objectives of evolving networks. In this paper, we investigate massive MIMO with HetNet, where the intended macro BS signal follows Ricean fading and interfering Femto BS signals follow Rayleigh fading. Subject to the Ricean assumption, strong line-of-sight (LOS) channel exists in the coverage area, when the high power macro BS is mounted at a high altitude. Then, by exploiting matrix and stochastic geometric tools, we evaluate the signal-to-interference (SIR). And obtain QOS objectives: coverage and outage probabilities, and area spectral efficiency (ASE). Further, we investigate the role of multiple antenna system in improving the SIR. This involves massive MIMO beamforming coordination of the macro BSs through power control with max-min optimization for users at the cell-edge. Numerical results show that the coverage and outage performance converge for different user locations, pathloss and Ricean factor. Also, the monotonic increase in Ricean factor improves the SIR of a user located within coverage region. That is, a user is in an outage at a distance where the Ricean factor is very small. And, optimal macro BS antennas and Ricean factor that achieve the ASE performance guarantee a rate-fairness between the cooperating macrocells, and avoid strong Ricean channel correlation. The performance gain is dependent on Ricean factor and user location, but independent of cell size.

Keywords: Massive MIMO, Ricean Fading, Beamforming, Stochastic Process, Heterogeneous Network, Interference Coordination, Spectral Efficiency

---

1. Introduction

The next generation wireless networks are to support the growing demands for high data rate especially over the network area. These demands require efficient modeling of the network design. Traditionally, cellular networks assume hexagonal, circular and square shape topologies, with the base station (BS) at the center of the cell. But these assumptions have some flaws in practical network designs. Recent network design in urban and suburban areas require random clustering [1], which has necessitated the redesigning of the traditional cellular networks.

Now, wireless network is heterogeneous, such that the small cells are offloading the macrocell, thereby improving the cell-center, cell-edge and indoor performance. Heterogeneous Networks (HetNets) are envisioned to provide the solution with: fast, flexible, cost efficient, fine tuned design and network expansion for the traditional cellular network architecture [2]. The base stations (BSs) in HetNets are characterized by the transmit power: different low-power BSs (Pico, Femto Access Points, micro) in addition with traditional high-power macro base-station (MBS) to improve on the coverage. The tiers consisting of BSs are ordered with the transmit power such that the served tier provides the highest signal power [3,4]. Thus, the tier's BSs transmit power, fading, path loss and

Peer-reviewed version available at Electronics 2018, 7, 79; doi:10.3390/electronics7060079

resource allocation. The scheduled users in HetNet connect to BSs from which strong propagation signal is received, and this includes connecting to neighboring tier's BSs. But the neighboring tier's BSs generate severe interference which is a limiting factor for the signal-to-interference (SIR) in achieving the network throughput [5,6]. This requires new approach to manage or reduce the interference.

1.1. Related Works

In recent times, random matrix theory [8] and stochastic geometry are used to study the characteristics of the SINR distribution and the performance gain of massive MIMO HetNet systems [9,10]. The enrichment of stochastic model in massive MIMO HetNet takes into account the distribution of BS locations and propagation model[1]. But the coexistence of the multiple and different BSs generate interference signals. Interference and user-centric analysis of massive MIMO HetNet is comprehensively discussed in [5,6,11,12], where the SINR is modeled over the locations of the users, BSs and characterized by multi-path fading. Incorporating multi-path fading into the point process model [13], the path loss with the fading can be geometrically characterized. And the coverage performance is conditioned on the user location over the entire network [14,15]. This primarily requires efficient analysis of the channel fading. The trade-off between the link reliability and area spectral efficiency (ASE) in multiuser MIMO HetNet is discussed in [12].

However, for BSs equipped with multiple antennas, precoding and beamforming can be exploited. The benefit of multiple antennas can be exploited in terms of multiplexing gain, diversity gain, and interference avoidance and Reduction. With massive MIMO Beamforming, the transmited signal energy can be directed toward the intended user in order to avoid and reduce interference to other users. Then, massive MIMO channel can therefore propagate jointly with both non-LOS (NLOS) and LOS channel. Such that the phases and transmit powers are combined, thus the mean power of the Ricean fading channel is obtained [7]. The performance of massive MIMO HetNet can be analyzed in the uncorrelated Rayleigh channel and uncorrelated Ricean MIMO channel.

Thus, massive MIMO HetNet have been studied in [16,17] for uplink and downlink deployment, respectively, under Rayleigh channel fading. In [18,19], the average rate performance over generalized fading channels are analyzed, where desired and interfering signals are separately deduced with different fading models such as Rayleigh and Nakagami fading. Also in [3,16], the channels are modeled with Rayleigh fading, these works analyzed both the desired and interfering signals of the downlink SINR with Rayleigh fading model. But assuming that all the propagation channels are dominated with NLOS transmissions within a cell is practically unrealistic. Therefore, the authors in [20] studied the general performance analysis with the path loss of the LOS and NLOS signal. An analytical approach for evaluating the coverage probability of HetNet with the desired propagation signals modeled with Ricean fading and interfering propagation signals modeled with Rayleigh fading, is recently introduced in [21]. This is due to the fact that the signal strength deteriorates at the cell edge as propagation enters the shadowed region, where dominate LOS is difficult to exist. As such the interfering signals at the location of a typical user are dominated with scattering signals [1]. But, owing to the complexity in analyzing Ricean distribution, especially the difficulty in approximating the Bessel function, majority of present contributions in literature [11,12,17–19,22–24] have focused on Rayleigh distribution for the coverage and outage probabilities. In [21], the authors analyzed coverage probability with Ricean and Rayleigh distributions for desired and interfering signals, respectively, while the authors in [25–27] investigated the performance Device-to-Device underlaid network and determined the effect of the channel propagations parameter of the Ricean Channel.

And, resource allocation in massive MIMO HetNet deployment involves bandwidth (frequency/time) management to mitigate interference, the user is allocated a portion of the spectrum

[1] In practice, the occurrence of random fading due to scattered and Line of sight (LOS) signals depend on the environmental factors such as distance, geographical structure and clutters.

Peer-reviewed version available at Electronics 2018, 7, 79; doi:10.3390/electronics7060079

in a sub-frame which indicates the entire spectrum in some time slots. Hence multiuser downlink transmit beamforming arises in resource allocation. Massive MIMO beamforming coordination involves transmit power control while maintaining user-fairness in certain threshold of SIR, thus maximizing the overall SIR [28,29]. Beam partition base on the BS sectors control is discussed in [30], where beam direction is used to control interfering BSs. By applying this interference management, the BSs can allocate the resources according to user selection criteria. Now, fractional frequency reuse (FFR) is designed to classify the scheduled users into the cell-center and cell-edge depending on the user-to-BS distance, thus accomplishes the power control, FFR is studied in [23,31]. All these related works under reasonable assumptions and objectives reduced the theoretical results to simple close-form expressions, to satisfy the future wireless networks.

Table 1. Summary of Related Works

Study	Theorem	Objectives	Propagation	Reference
HetNet	Stochastic	Throughput EE, ASE, SIR Distribution Coverage and Outage probability	Rayleigh ——— Ricean	[3,9,11][12]^{M}[13,15,18,19,22][23]^{M}[24][29]^{M}[31] ——— [14,21][25–27]^{D}

*M is Massive MIMO systems approach
*D is Device-to-Device communications approach

1.2. Problem statement

Many works (in the Summary of Related works table) have studied the performance of HetNet with Rayleigh fading, as it is easier to analyze the fading distribution. Realistically, mounting macro BS on high elevation for wide coverage, LOS and NLOS signals can be exploited, thus Ricean channel is realized. While the small cell BSs have small coverage, hence generate strong scattering signals outside the coverage range. Then from the ideas in [1,21], this work develops a HetNet model and analytically characterizes the SIR with Ricean and Rayleigh fading distributions. That is, we evaluate the SIR with the convolution of the desired signal (from macro BS) with Ricean distribution and interfering signals (from femto BSs) with Rayleigh distribution. And, massive MIMO is considered for modeling the fading channels, this is a novel contribution in this work. We study the SIR distribution by analyzing the geometry users, Ricean fading distribution and transmit power allocation. Further, we propose transmit power control technique for the downlink beamforming coordination.

1.3. Contributions of the paper

This work studies a downlink massive MIMO HetNet with the macro cells employing Ricean fading and the SCN using Rayleigh fading. Thus below are major contributions:

- We use the fading distributions to evaluate the intended signal (Ricean fading) and interfering signals (Rayleigh fading)
- We provide a tractable expression of the typical user SIR and evaluate the probability of coverage, outage probability and area spectral efficiency (ASE).
- To further improve on the location-dependent user's QOS, we introduce FFR scheme for interference coordination which is used to analyze cell-edge users performance. Then to avoid spill-over of power by the high power macro-cell, we propose massive MIMO beamforming coordination among the macro BSs through power control.
- Finally, we obtain optimal values for BS antennas and Ricean factor that helps to avoid the strong LOS channel correlation.

Preprints (www.preprints.org) | NOT PEER-REVIEWED | Posted: 3 May 2018 doi:10.20944/preprints201805.0072.v1

Peer-reviewed version available at Electronics 2018, 7, 79; doi:10.3390/electronics7060079

2. System Design

2.1. General Description

In this section, the users and BSs are associated in the Voronoi cell with the coverage areas comprising of Voronoi tessellation. And the network is assumed to be open access, a user can access any tier's BSs in the service area [4] and each user is served by the nearest BS, thus interference is generated to a user who is outside the respective tier. Then, by spatial stochastic process with the Poisson point model, the femto cells are irregularly setup whilst the macrocell BSs are regularly setup (cf. Figure 1). Now, assuming all the BSs are transmitting, a macrocell user receives interference induced by the femto cells. Also, all the BSs share a common frequency band for communications. Adopting orthogonal frequency in the downlink LTE system, the available frequency per tier are partitioned into sub-bands of the subcarrier. The users that connect to the under study tier BSs have no intra-tier interference since intra-tier interference occurs from co-channel neighboring same tier BSs, thus we assume coordination among the macrocell BSs. Whereas no coordination with the femtocells, since the femtocell deployments are random and uncontrolled. Again, we assume no coordination between macro BS and femto BS, then inter-tier interference is from femto BS to the macro cell user. However in dense network, the macrocell user experiences both dominant line of sight (LOS) and scattered signal propagations from macro BS, while signals from femtocell BS are likely to be only scattering. By this propagation assumption, the network is designed such that user to BS association and received power weakness strive on the user location.

Assumption 1: *In this analysis, we assume the desired (intended) signal follows Ricean fading distribution whilst the interfering signals follow Rayleigh fading distribution with sufficient scattering*.

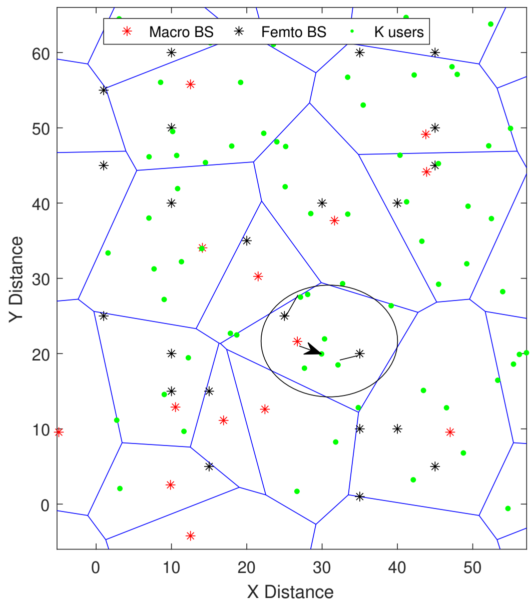

Figure 1. The plot models the system design with the understudy cluster having circle wrap around it, the arrow line is the dominant LOS signal to scheduled user.

2.2. Poisson point Process model

We consider downlink massive MIMO HetNet consisting of two tiers, that is nth and jth tiers are macro and femto cells respectively. In the nth tier, the BSs are spatially distributed according to independent homogeneous Poisson point Process (PPP) Φ_n with density λ_n, bounded in area of

Preprints (www.preprints.org) | NOT PEER-REVIEWED | Posted: 3 May 2018 doi:10.20944/preprints201805.0072.v1

Peer-reviewed version available at *Electronics* **2018**, *7*, 79; doi:10.3390/electronics7060079

$A_n \subset \mathbb{R}^2$, as $\Phi_n(A) \sim PPP(\lambda_n)$. Each BS in the n tier has equal transmit power P_n, M transmit antennas. We assume K single antenna users spatially distributed over $\mathbb{R}^2$ in a homogeneous PPP Φ_u.

2.3. Channel Model and Beamforming Design

Considering MIMO HetNet with the intended signal from the nth tier (macro BSs), then typical user receives interference from BSs of the jth tier (femto BS). The small-scale fading of the desired and interference signals are given in Ricean fading $\mathbf{g}_n \in \mathcal{CN}(1_{M\times1}, \mathbf{I}_M)$ and Rayleigh fading $\mathbf{g}_j \in \mathcal{CN}(0_{M\times1}, \mathbf{I}_M)$, respectively. Now, massive MIMO beamforming is used in this model to surmount signal propagation loss, so the transmitted signal for the nth tier BS is $\mathbf{z}_n = \sum_{i=1}^{\Phi_u} \mathbf{w}_{n,i} s_{n,i} \in \mathbb{C}^{M\times1}$, where $\mathbf{w}_{n,i}$ and $s_{n,i}$ are the beamforming vector and information signal for the ith user respectively. Then, employing the MR transmit beamforming with perfect CSI at transmitter, the columns of the beamforming matrix $\mathbf{W}_n = [\mathbf{w}_{n,i}]_{1\le i\le\Phi_u} = \tilde{\mathbf{G}}_n^* \in \mathbb{C}^{M\times\Phi_k}$, with $\tilde{\mathbf{G}}_n = [\tilde{\mathbf{g}}_1, .., \tilde{\mathbf{g}}_i, ..\tilde{\mathbf{g}}_{\Phi_u}]^* \in \mathbb{C}^{\Phi_k\times M}$, for $\tilde{\mathbf{g}}_n = \frac{g_i}{\|g_i\|}$ is the normalized channel direction to the user. And the intended channel power for user located at x_o is $h_{n,x_o} = \left|\mathbf{g}_{n,x_o}^* \mathbf{w}_n\right|^2$, where the channel power follows Gamma distribution which is given as $h_{n,x_o} \sim \Gamma(M, 1)$ [1]. In the interfering marks, the beamforming matrices have unit-norm orthogonal columns, the interfering channel vector $\mathbf{g}_{j,x} \in \mathbb{C}^{\Phi_u\times1}$ and beamforming vector $\mathbf{w}_j$ are independent unit-norm random vectors. So, interfering channel power $h_{j,x} = \left|\mathbf{g}_{j,x}^* \mathbf{w}_j\right|^2$ follows Gamma distribution as $h_{j,x} \sim \Gamma(1, 1)$, since beamforming vectors $\mathbf{w}_j$ have no clear angular directivity, hence the channel vectors are estimated from independent $\mathbf{g}_{j,x}$. The interferers are modeled as complex Gaussian with zero mean and unit variance, the variance depends on the channel fading and user locations. This implies the statistical order of interferers depend on the pathloss attenuation and transmission characteristics.

2.4. The Fading Distribution

The elements of the channel fading are i.i.d complex Gaussian with two independent random variables. And the distribution of the elements have magnitudes by the probability density function (pdf). Now, focusing on the averaged received power rather than the magnitude, the pdf of average received power with Rayleigh fading is given as

$$f_{P_r}(z) = \frac{z}{P_r} \exp\left(-\frac{z^2}{P_r}\right) \qquad z \ge 0 \tag{1}$$

where P_r is the averaged received power. But, assuming LOS channel exists between the BS and the user, the total power associated with the channel coefficient is shared between the LOS and the scattering channels. Let variance σ_{n,x_o}^2 be the average power of the channel $\mathbf{h}_{n,x_o}$. We define Ricean factor as $\kappa = \frac{\sigma_{LOS}^2}{\sigma_{n,x_o}^2}$, where $\sigma_{LOS}^2 = \kappa\sigma_{n,x_o}^2$, and channel power is [32]

$$h_{n,x_o} = \sqrt{\sigma_{n,x_o}^2 \kappa} + \Omega \tag{2}$$

where Ω denotes the real and imaginary parts of the fading signal which are statistically independent zero-mean Gaussian variable with σ_{n,x_o}^2 variance. Then the channel power becomes

$$P_r = (\kappa + 1)\, \sigma_{h_{n,x_o}}^2 \tag{3}$$

Then, the pdf of average received channel power with Ricean fading is formulated as

$$f_{P_r}(z) = \frac{2(\kappa+1)z}{P_r} \exp\left(-\kappa - \frac{(\kappa+1)z^2}{P_r}\right) I_0\left(2\sqrt{\frac{\kappa(\kappa+1)z^2}{P_r}}\right) \qquad z \ge 0 \tag{4}$$

Peer-reviewed version available at Electronics 2018, 7, 79; doi:10.3390/electronics7060079

where $I_0(\cdot)$ is the modified zero-th order Bessel function of the first kind. Note that z is independent of the Ricean factor κ, so for $\mathbb{E}[z]=1$, then the Laplace transform is given as

$$\mathbb{E}[\exp(-zs)] = \frac{(\kappa+1)}{(\kappa+1)+s}\exp\left(-\frac{\kappa s}{(\kappa+1)+s}\right) \tag{5}$$

thus (5) decreases with κ for any s. On the other hand, increasing the κ can also increase any average metric that obeys the completely monotonic function [13]. There are other fading distributions (e.g. Nakagami distribution) in wireless communications [18,19,33].

3. The SIR distribution

Now, the received signal from nth tier BS at the typical user located at the origin o is given as

$$y_{n,o} = \sqrt{p_n}\left\|x_o\right\|^{-\frac{\alpha_o}{2}}\mathbf{g}^*_{n,x_o}\mathbf{z}_n + \sum_{x\in\Phi_j\setminus x_o}\sqrt{p_j}\left\|x\right\|^{-\frac{\alpha_j}{2}}\mathbf{g}^*_{j,x}\mathbf{z}_j \tag{6}$$

where α_o and α_j denote the intended signal and interfering signal pathloss exponents, respectively, $\|\cdot\|$ is the Euclidean norm and p_n is the average transmit power per BS. In interference limited system, the thermal noise power is negligible with respect to the interference power. The received power of the typical user at the origin from the association metric [5] is given as

$$\begin{aligned} P_{n,o} &= p_n h_{n,x_o}\left\|x_o\right\|^{-\alpha_o} \\ &= p_n h_{n,o} r_o^{-\alpha_o} \end{aligned} \tag{7}$$

where $r_o^{-\alpha} = \|x_o\|^{-\alpha}$ models distance path-loss effect in the standard power law. Then, the resulting signal to interference ratio (SIR) of the user served by BS at location r_o in the nth tier is given as

$$\varphi_{n,o} = \frac{p_n h_{n,o} r_o^{-\alpha_o}}{\sum_{r_j\in\{\Phi_j\setminus r_o\}} p_j h_j r_j^{-\alpha_j}} \tag{8}$$

With (8), the typical user connects to the BS that provides the strongest instantaneous received power, and accesses the optimum transmit BS antennas. For macro BS equipped with M antennas, each user receives M SISO subchannels. And, the Ricean channel $\mathbf{g}_n \in \mathcal{CN}\left(1_{M\times 1}, \mathbf{I}_M\right)$ follows specific pdf, where the mean of the non-central distribution is equivalent to M antennas. Because the largest eigenvalue in the non-central case grows unbounded along the rank of the channel matrix [34]. Then, Ricean channel have deterministic mean κM known for beamforming, hence (2) is rewritten as $h_{n,o} = \kappa M + 1$. Therefore in (7), $P_{n,o} = (\kappa M + 1)\, r_o^{-\alpha}$ is the average power received of the Ricean signal. Then, we can rewrite received power of the Ricean pdf (4) with the QOS threshold T_n, for $\varphi_{n,o}(r_o) \geq T_n$ as

$$f_{P_r}\left(T_n/r_o\right) = \exp\left(-\kappa M - T_n r_o^{\alpha_o}\right) I_0\left(2\sqrt{\kappa M T_n r_o^{\alpha_o}}\right) \tag{9}$$

Further, by setting the Bessel function transformation $I_0(a) = \sum_{m=0}^{\infty}\frac{\left(\frac{a}{2}\right)^{2m}}{(m!)^2}$, we rewrite (9) as

$$f_{P_r}\left(T_n/r_o\right) = \exp\left(-\kappa M - T_n r_o^{\alpha_o}\right)\sum_{m=0}^{\infty}\frac{\left(\kappa M T_n r_o^{\alpha_o}\right)^m}{(m!)^2} \tag{10}$$

where the positive integer order m gives the factional moments of the received power. The Ricean received power reduces to Rayleigh as $f_{P_r}\left(T_n/r_o\right) = \exp\left(-T_n r_o^{\alpha_o}\right)$ when $\kappa = 0$. Note that the m infinite series of the (i.i.d) Ricean channel entries have same Ricean factor κ in the non-central chi-square pdf's [7]. Figure (2) verifies some values of m with the Ricean factor. The m infinite series expression in

Preprints (www.preprints.org) | NOT PEER-REVIEWED | Posted: 3 May 2018 doi:10.20944/preprints201805.0072.v1
Peer-reviewed version available at Electronics 2018, 7, 79; doi:10.3390/electronics7060079

(10) converges when m becomes large, the convergence is $\left(\kappa M T_n r_o^{\alpha_o}\right)$ dependent. Therefore for large Ricean factor $\kappa \rightarrow \infty$, the pdf turns to be more narrow and reduces to approach a Dirac impulse, which corresponds to no fading condition.

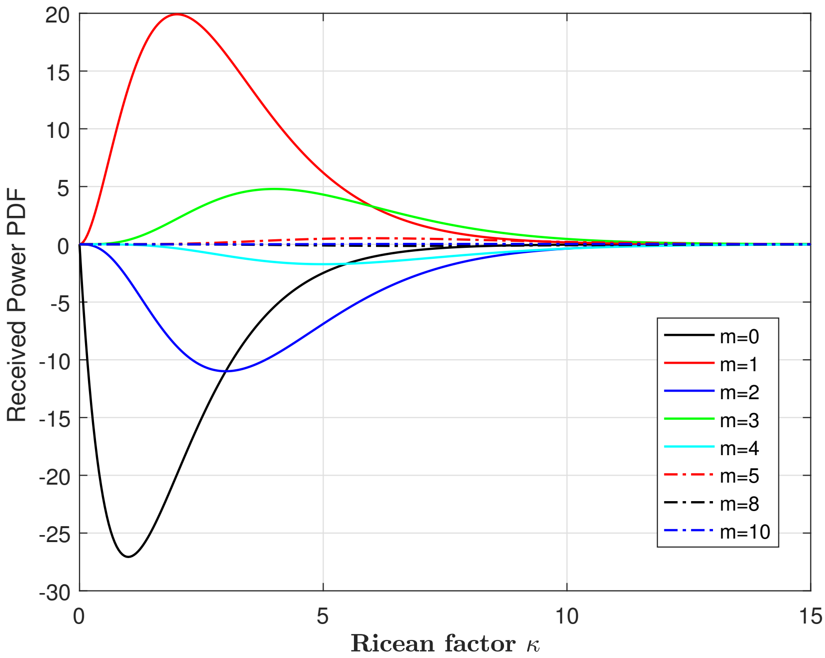

Figure 2. Convergence of the infinite series with values of the Ricean factor for the modified Bessel function of the first kind

3.1. Intended Signal Power

For uniformly distributed users over an infinite range of R, the users are associated by distance probability w.r.t the serving BSs. We obtain the pdf $f_R\left(r_o\right)$ for user to serving macro BS distance as [16]

$$f_R\left(r_o\right) = \begin{cases} \frac{2r_o}{R^2} & \text{for } r_o \in [0,\ R] \\ 0 & \text{otherwise} \end{cases} \tag{11}$$

From (10) and (11), we can determine the distribution of received power for the intended user with Ricean fading at location r_o, this can be expressed as

$$\begin{aligned} P_{r,o}\left(T_n/r_o\right) &= \int_0^R f_{P_r}\left(T_n/r_o\right) f_R\left(r_o\right) dr_o \\ &= \frac{2\exp\left(-\kappa M\right)}{R^2} \sum_{m=0}^{\infty} \frac{\left(\kappa M T_n\right)^m}{\left(m!\right)^2} \int_0^R r_o^{\alpha_o m+1} \exp\left(-T_n r_o^{\alpha_o}\right) dr_o \\ &\overset{(d)}{=} \frac{2\exp\left(-\kappa M\right)}{\alpha R^2} \sum_{m=0}^{\infty} \frac{\left(\kappa M\right)^m}{\left(m!\right)^2} \frac{T_n^m}{T_n^{m+\frac{2}{\alpha_o}}} \int_0^{T_n} t^{m+\frac{2}{\alpha_o}-1} \exp\left(-t\right) dt \\ &\overset{(e)}{=} \frac{2\exp\left(-\kappa M\right)}{\alpha_o R^2 T_n^{\frac{2}{\alpha}}} \sum_{m=0}^{\infty} \frac{\left(\kappa M\right)^m}{\left(m!\right)^2} \gamma\left(m + \frac{2}{\alpha_o}, T_n\right) \\ &\overset{(f)}{=} \frac{2\exp\left(-\kappa M\right)}{\alpha_o R^2} \sum_{m=0}^{\infty} \frac{\left(\kappa M\right)^m}{\left(m!\right)^2 \left(m + \frac{2}{\alpha_o}\right)} T_n^m e^{-T_n} \end{aligned} \tag{12}$$

Preprints (www.preprints.org) | NOT PEER-REVIEWED | Posted: 3 May 2018 doi:10.20944/preprints201805.0072.v1

Peer-reviewed version available at Electronics 2018, 7, 79; doi:10.3390/electronics7060079

where step(d) follows from a lower incomplete Gamma function with the integral function $\int_0^u x^m \exp\left(-\beta x^n\right) dx = \frac{\gamma(v)}{n\beta^v}$ ([35], eqn. 3.381 8), $\gamma\left(\cdot\right)$ is the lower incomplete gamma function given in step(e) as $\gamma\left(a, x\right) = \int_0^x t^{a-1} \exp\left(-t\right) dt$ ([35], eqn. 8.350 1) and step(f) follows from the relation $\gamma\left(a+b, x\right) = \frac{1}{a+b}\left[\Gamma\left(a+b+1, x\right) + x^{a+b}e^{-x}\right]$ ([35], eqn. 8.355 9). And setting $c = a+b+1$, then adopting $\Gamma\left(c, \infty\right) = 0$ ([35], eqn. 8.350 4), with $T_n \geq 0$ arrives at step (f). Furthermore, the cumulative distribution function (CDF) of the intended received power is given as

$$\begin{aligned} F_{r,o}\left(T_n/r_o\right) &= \int_0^{\infty} P_{r,o}\left(T_n\right) dT_n \\ &= \frac{2\exp\left(-\kappa M\right)}{\alpha_o R^2\left(k+\frac{2}{\alpha_o}\right)} \sum_{m=0}^{\infty} \frac{\left(\kappa M\right)^m}{\left(m!\right)^2} \int_0^{\infty} T_n^m e^{-T_n}\, dT_n \\ &\overset{(a)}{=} \frac{2\exp\left(-\kappa M\right)}{\alpha_o R^2\left(m+\frac{2}{\alpha_o}\right)} \sum_{m=0}^{\infty}\sum_{k=0}^{m} \frac{\left(\kappa M\right)^m}{\left(m!\right)^2} \left(-1\right)^k k! \binom{m}{k} e^{-T_n} T_n^{m-k} \end{aligned} \tag{13}$$

where step (a) follows from ([35], eqn. 2321 2). In (13), the performance of specific user depends on the mobility and pathloss, with $\left(\alpha_o > 2\right)$ fulfilling practical network design.

3.2. Interference Signal power

Now, with interference from the jth tier BSs, we define $R_j = \frac{P_j}{r_j^{\alpha_j}}$ as the average received pathloss power from all interferers. So, pdf of the interferers power over Rayleigh distribution (1) is written as

$$f_{P_r}\left(T_n/r_j\right) = \frac{1}{R_j} \exp\left(-\frac{T_n}{R_j}\right) \tag{14}$$

Assuming independent and identically distributed interferers, the CDF of the interfering powers can be computed in closed form with Laplace transform. The Laplace transform of the aggregated interference power (14) in the jth tier BSs is given as

$$\begin{aligned} L_{I_j}(s) &= \mathbb{E}_{I_j}\left[\exp\left(-sI_j\right)\right] \\ &= \int_0^{\infty} \mathbb{E}_{I_j}\left[\exp\left(-s \sum_{r_j \in \left\{\Phi_j \backslash r_o\right\}} T_n\right) \times \prod_{j \in \Phi_j} P(T_n/r_j) dT_n\right] \\ L_{I_j}(s) &\overset{(a)}{=} \mathbb{E}\left[\prod_{r_j \in \left\{\Phi_j \backslash r_o\right\}} \frac{1}{1+sR_j}\right] \end{aligned} \tag{15}$$

where step(a) follows from the independence of the exponential Rayleigh fading. The locations of the interferers are evaluated by the probability generating functional (PGFL) of PPP, that is $\mathbb{E}\left[\prod_{x\in\Phi} f\left(x\right)\right] =$

Preprints (www.preprints.org) | NOT PEER-REVIEWED | Posted: 3 May 2018 doi:10.20944/preprints201805.0072.v1

Peer-reviewed version available at Electronics 2018, 7, 79; doi:10.3390/electronics7060079

$\exp\left(-2\pi\lambda\int_{R^2} 1 - f\left(x\right)dx\right)$ [24]. Thus, the total interfering signal is conditioned by the typical user at location r_o to the serving BS. Therefore, putting $s = T_n r_o^{\alpha_o}$ into (15), we get [19,24]

$$
\begin{aligned}
f_{I_j}\left(r_o\right) &= \exp\left(-2\pi\lambda_n \int_{R^2} 1 - \frac{1}{1 + T_n r_o^{\alpha_o} R_j} r_j dr_j\right) \\
&= \exp\left(-2\pi\lambda_n \int_{r_o} \frac{1}{1 + \left(T_n r_o^{\alpha} \frac{P_j}{r_j^{\alpha_j}}\right)^{-1}} r_j dr_j\right) \\
&= \exp\left(-2\pi\lambda_n \int_{r_o} \frac{1}{1 + \left(\frac{r_j}{T_n^{\frac{1}{\alpha_j}} P_j^{\frac{1}{\alpha}} r_o^{\frac{\alpha_o}{\alpha_j}}}\right)} r_j dr_j\right) \\
&\stackrel{(a)}{=} \exp\left(-\pi\lambda_n T_n^{\frac{2}{\alpha_j}} P_j^{\frac{2}{\alpha_j}} r_o^{2\left(\frac{\alpha_o}{\alpha_j}\right)} \int_{T_n - \frac{2}{\alpha_j}}^{\infty} \frac{1}{1 + (u)^{\frac{\alpha_j}{2}}} du\right) \\
&= \exp\left(-\pi\lambda_n P_j^{\frac{2}{\alpha_j}} r_o^{2\left(\frac{\alpha_o}{\alpha_j}\right)} \rho\left(T_n, \alpha_j\right)\right)
\end{aligned} \tag{16}
$$

where step (a) follows from the standard pathloss model. The aggregated interferers power is received by the typical user at location r_o to a serving BS which is associated to nth tier. But transmit power P_j creates power imbalance between the macroBS and femtoBS.

4. Performance Metric

Here, a typical user is within coverage when the received SIR from the set of serving BSs is greater than the threshold SIR. So, the instantaneous mutual information is captured in the fading channel within the SIR, the probability of outage is formulated as

$$\mathbb{P}_{\{\text{out}\}}(r_o) = \mathbb{P}\left(\varphi_o(r_o) \geq T_n\right) = 1 - \mathbb{P}_{\{\text{cov}\}}(r_o) \tag{17}$$

where $\varphi_o(r_o)$ is instantaneous SIR for user located at r_o and $\mathbb{P}_{\{\text{cov}\}}(r_o)$ is the probability of coverage that ensures SIR $\varphi_o(r_o)$ is above the T_n, this helps to evaluate the spectral efficiency at the cell edge. The second performance metric is based on the Shannon throughput $\log_2\left(1 + \varphi_o(r_o)\right)$, we formulate the downlink average area spectral efficiency (ASE) as

$$ASE = \Phi_k \lambda_n \left[\log\left(1 + T_n\right)\right] \mathbb{P}_{\{\text{cov}\}}(r_o) \tag{18}$$

For simplicity of our analysis, we assume all the tiers have the same quality of service threshold. The most important network performance parameters are: $\{\lambda_n, r_o, M, K, \kappa, P_n, T_n\}$.

4.1. Coverage Probability

The coverage probability $\mathbb{P}\left(\varphi_o(r_o) \geq T_n\right)$ is achieved by evaluating the complementary CDF (CCDF) of the intended received power $F_{r,o}\left(T_n/r_o\right)$, in relation with specific knowledge of aggregated interfering power $f_{I_j}(r_o)$ [27] in accomplishing the target user SIR.

Peer-reviewed version available at Electronics 2018, 7, 79; doi:10.3390/electronics7060079

Theorem 1. *For a typical user conditioned at r_o to a BS associated with nth tier, the probability of coverage for intended signal experiencing Ricean fading, and interfering signals experiencing Rayleigh fading is given as*

$$\mathbb{P}\{cov\}(r_o) = \frac{2\exp\left(-\kappa M\right)}{\alpha_o R^2} \sum_{m=0}^{\infty} \sum_{k=0}^{m} (-1)^k k! \binom{m}{k} \frac{(\kappa M T_n)^m}{(m!)^2 \left(m + \frac{2}{\alpha_o}\right) T_n^k} \frac{d^{m-k} L_{I_j}(r_o)}{d T_n^{m-k}} \tag{19}$$

Proof. By expression, the probability of coverage associated with the SIR, is obtain from the convolution relation of the CCDF's of desired and interfering signals. This approach differs from existing approach in [1,2,16,24]. We formulate the convolution from (13) and (16) as $\mathbb{P}\{\text{cov}\}\left(r_o\right) = \int_0^\infty F_{r,o}\left(T_n/r_o\right) f_{I_j}(r_o) dr_o$ [21], then we deduce the convolution as

$$\begin{aligned}
\mathbb{P}\{\text{cov}\}\left(r_o\right) &= \frac{2\exp\left(-\kappa M\right)}{\alpha_o R^2} \sum_{m=0}^{\infty} \sum_{k=0}^{m} \frac{(\kappa M)^m}{(m!)^2 \left(m + \frac{2}{\alpha_o}\right)} (-1)^k k! \binom{m}{k} \int_0^\infty \left(T_n r_o\right)^{m-k} e^{-T_n r_o} f_{I_j}(r_o) dr_o \\
&= \frac{2\exp\left(-\kappa M\right)}{\alpha_o R^2} \sum_{m=0}^{\infty} \sum_{k=0}^{m} \frac{(\kappa M T_n)^m}{\left(m + \frac{2}{\alpha_o}\right) (m!)^2 T_n^k} (-1)^k k! \binom{m}{k} \int_0^\infty r_o^{m-k} e^{-T_n r_o} f_{I_j}(r_o) dr_o \\
&\overset{(a)}{=} \frac{2\exp\left(-\kappa M\right)}{\alpha_o R^2} \sum_{m=0}^{\infty} \sum_{k=0}^{m} \frac{(\kappa M T_n)^m}{\left(m + \frac{2}{\alpha_o}\right) (m!)^2 T_n^k} (-1)^k k! \binom{m}{k} \frac{d^{m-k} L_{I_j}(r_o)}{d\left(T_n\right)^{m-k}}
\end{aligned} \tag{20}$$

□

where step(a) follows from Laplace transformation derivatives with piecewise continuous function of exponential order, which takes the form $\frac{dF}{ds} = -\int_0^\infty t f(t) e^{-st} dt = -L\left|\left[t f\left(t\right)\right]\right|_s$. According to the completely monotonic function $(-1)^n \frac{d^n g(x)}{dx^n} \geq 0$ [13], the nth order differentiable is as $L\left|\left[t^n f\left(t\right)\right]\right|_s = (-1)^n \frac{d^n F}{ds^n}$, thus we can define $\frac{d^{m-k} L_{I_j}(r_o)}{d(T_n)^{m-k}} = (-1)^{m-k} \int_0^\infty r_o^{m-k} e^{-T_n r_o} f_{I_j}(r_o) dr_o$, this completes the proof.

4.2. Area Spectral Efficiency

Consider CSI available at both transmitter and receiver, the transmitter adapts to the transmission strategy of the channel fading with the receiver. The spectral efficiency is lower bounded on the average capacity for small asymptotic probability of error over the user location. Thus, the area spectral efficiency (18) over the distance r_o can be formulated by

$$ASE = \Phi_u \lambda_n \mathbb{P}_{\{\text{cov}\}}(r_o) \int_0^\infty \mathbb{E}\left\{\ln\left(1 + \varphi_o(r_o)\right)\right\} dr_o \tag{21}$$

where $\mathbb{P}_{\{\text{cov}\}}(r_o)$ is the coverage probability which is herein considered for analytical and simulation comparison. In (21), we define the area spectral efficiency over the SIR distribution in relation with user location. From (17) and (18), the SIR is $(\varphi_o(r_o) \geq T_n)$, with T_n as the minimum limit for the target SIR. Since (21) is non-negative variable, we determine the average rate by the equivalent combination over the user location and fading distribution as

$$\begin{aligned}
\int_0^\infty \mathbb{E}\left\{\ln\left(1 + \varphi_o(r_o)\right)\right\} dr_o &\overset{(a)}{=} \int_0^\infty \ln\left(1 + y\right) f_{\varphi_o/r_o}\left(y\right) dy \\
&\overset{(b)}{=} \int_0^\infty \frac{\mathbb{P}\{\text{cov}\}(y)}{(1+y)} dy \\
&\overset{(c)}{=} \int_0^\infty \mathbb{P}\{\text{cov}\}(\exp(t) - 1) dt
\end{aligned} \tag{22}$$

where step (a) follows from $f_{\varphi_o/r_o}\left(y\right) dy$ as the envelope of fading distribution w.r.t SIR, step (b) follows from the CDF of $f_{\varphi_o/r_o}\left(y\right) dy$ as $F_{\varphi_o/r_o}(y) = 1 - \mathbb{P}\{\text{cov}\}(y)$. Then applying

Preprints (www.preprints.org) | NOT PEER-REVIEWED | Posted: 3 May 2018 doi:10.20944/preprints201805.0072.v1

Peer-reviewed version available at Electronics 2018, 7, 79; doi:10.3390/electronics7060079

the integration by part given as $-\ln(1+y)\left(1-F_{\varphi_o/r_o}(y)\right)+\int_0^\infty \frac{1}{(1+y)}\left(1-F_{\varphi_o/r_o}(y)\right)dy$, for $-\ln(1+y)\left(1-F_{\varphi_o/r_o}(y)\right)=0$, step(c) follows by setting $t=\ln(1+y)$, therefore plugging (22) into (21), we arrive at

$$\begin{aligned} ASE &= \frac{\Phi_u}{\ln(2)}\lambda_n \int_0^\infty \mathbb{P}\{\text{cov}\}(\exp(t)-1)dt \\ &\overset{(a)}{=} \frac{\Phi_u}{\ln(2)}\lambda_n \sum_{m=0}^{\infty}\sum_{k=0}^{m}(-1)^{k-2}\int_{t>0}\frac{(\exp(t)-1)^{k-2}}{k!}\frac{d^{k-2}L_{I_r}((\exp(t)-1)r_o^{\alpha})}{d(T_n)^{k-2}}dt \end{aligned} \tag{23}$$

where step (a) follows from substituting (19) and rearranging the terms, the integral is taken over non-negative integer t. Now in (23), the area spectral efficiency is evaluated with $\varphi_o(r_o)$ (8) over received power (7) at the user location and Ricean channel gain. Then, to further improve the overall performance, we design macro BSs cooperation approach to jointly control power in (7), especially at the cell edge. The next section focuses on developing a beamform coordination approach.

5. Macro-Cell Optimization and Coordination

In massive MIMO HetNet, the high power macro BS enhances the edge effects between adjacent macrocell. The finite range (11) of macro BS creates a process with macrocell users at cell-center receiving stronger channel power $P_{n,o}$ than at cell-edge. This calls for association metric for cell center or edge users by considering the fractional frequency reuse (FFR) [23,36]. Then, to guarantee QOS T_n for the macrocell user, a downlink coordinated massive MIMO beamforming is proposed. This involves individual power constraints through exploiting CSI to control the QOS requirements of the user [37]. As such, most favorable macrocell with path gain and power serves the user. The constraint provides the max-min optimality for the SIR T_n and user fairness (maximum worst-user SIR).

So, let the set of users served by n tier macro BSs be Φ_u, and $k \in \Phi_u$ is the index of user k served by of the macroBS at the origin r_o. Also transmit power p_k and beamforming vector $\mathbf{w}_k \in \mathbb{C}^{M\times 1}$. And the distance to the nearest macrocell BS as r, then the received SIR of user k is written as

$$\begin{aligned} \varphi_k(\mathbf{W},\mathbf{p}) &= \frac{p_k\left|\mathbf{g}_{ko}^{\dagger}\mathbf{w}_k\right|^2 r_o^{-\alpha_o}}{\sum_{r\in\Phi_n} p_r\left|\mathbf{g}_{kr}^{\dagger}\mathbf{w}_r\right|^2 r^{-\alpha_o}} \\ &= \frac{p_k\left|\mathbf{g}_{ko}^{\dagger}\mathbf{w}_k\right|^2 r_o}{\sum_{r\in\Phi_n} p_r\left|\mathbf{g}_{kr}^{\dagger}\mathbf{w}_r\right|^2 \beta_k} \end{aligned} \tag{24}$$

where $\beta_k = \left(\frac{r}{r_o}\right)^{-\alpha_o}$ and $\mathbf{g}_{ko}$ is the channel vector from macro BS o to user k, also $\mathbf{p} \triangleq [p_1, p_2 ..., p_{\Phi_k}]^{\mathrm{T}}$ and $\mathbf{W} \triangleq \mathrm{diag}(\mathbf{w}_1, \mathbf{w}_2 ..., \mathbf{w}_{\Phi_k})$ is the beamforming for the cluster of macro BS. The macro BS coordination regions β_k are different for different users. Thus, a user prefers to connect to BS with lowest pathloss, higher transmit power. The objective of the inter-cluster (macrocell) coordination is to jointly optimize the beamformer $\mathbf{w}_k$ and transmit p_k power. Then, the maxi-min optimization problem under weighted SIR [2] can be expressed as

$$\begin{aligned} &\max_{\mathbf{W},\mathbf{p}} \min_{k} \frac{\varphi_k(\mathbf{W},\mathbf{p})}{\varsigma_k} \geq \frac{T_n}{\varsigma_k} \\ &\text{s.t} \quad p_k \geq 0, \|\mathbf{w}_k\|^2 = 1 \end{aligned} \tag{25}$$

[2] The weighted QOS constraint indicates that the macro BSs form coordinated beamforming and power control so as to achieve the required fairness level for users within the macrocell cluster.

where ς_k ensures quality of service priority with SIR for the kth user. Large factor ς_k ensures higher SIR φ_k for that macrocell user. Herein, the optimization problem in (25) is non-convex, but base on [38], this can be shifted to the second-order cone programming (SOCP) problem [40] and implemented on MATLAB. The global optimal solution is achieved by convex optimization method. Next, we formulate the power minimizations problem as

$$\begin{aligned} &\min_{p_k, \mathbf{w}_k} \sum_{r \in \Phi_n} p_r \\ \text{s.t } &\frac{\varphi_k(\mathbf{W}, \mathbf{p})}{\varsigma_k} \geq \frac{T_n}{\varsigma_k} \\ &\|\mathbf{w}_k\|^2 = 1 \end{aligned} \tag{26}$$

Now, with the downlink and uplink duality, we define the uplink power q, then optimal beamformer can be defined by

$$\mathbf{w}_k^{opt} = \arg\min_{\mathbf{w}_k} \frac{\mathbf{w}_k^{\dagger} \left\{ \sum_{r \in \Phi_n} q_r \left(\mathbf{g}_{kr} \mathbf{g}_{kr}^{\dagger} \right) \right\} \mathbf{w}_k}{\mathbf{w}_k^{\dagger} \left(\mathbf{g}_{ko} \mathbf{g}_{ko}^{\dagger} \right) \mathbf{w}_k} \tag{27}$$

And, we develop the maximization problem of the T_n as

$$\begin{aligned} &\max_{\mathbf{W}, \mathbf{p}} \; T_n \\ &\frac{\varphi_k(\mathbf{W}, \mathbf{p})}{\varsigma_k} \geq \frac{T_n}{\varsigma_k} \qquad \forall_k \\ &p_k \geq 0, \\ &\|\mathbf{w}_k\|^2 = 1 \end{aligned} \tag{28}$$

where the slack variable T_n is maximize whereas all the SIRs are kept above the slack variable. The focus of coordination is that, only one macroBS can transmit full power whilst other macroBS transmit less power to reduce inter cluster effects, this guarantees fairness for cell-edge users. Hence the optimal transmit power that maximizes the achievable performance is user location dependent. We can write the algorithm as

Peer-reviewed version available at *Electronics* **2018**, *7*, 79; doi:10.3390/electronics7060079

Table 2. Algorithm for Max-Min Weighted SIR for Macrocell

Initiate $\mathbf{p}[\mathbf{0}]$, $\mathbf{q}[0]$, $\mathbf{w}[\mathbf{0}]$
For $t = 1, 2, 3, ...$until convergence, iterate below steps
repeat
1.From (26), update the uplink transmit power $\mathbf{q}[t+1]$

$$q_u[t+1] = \left(\frac{\varsigma_k}{\varphi_k\left(\mathbf{W}[\mathbf{t+1}], \mathbf{q}[\mathbf{t}]\right)}\right) q_k[t]$$

2.Update the transmit beamforming matrix $\mathbf{W}[t+1]$, as given (27):

$$\mathbf{w}_k[t+1] = \frac{p_u\left(\sum_{r\in\Phi_n}|\mathbf{g}_{kr}\mathbf{g}_{kr}^{\dagger}|\right)}{\left\|pu\left(\sum_{r\in\Phi_n}\mathbf{g}_{kr}\mathbf{g}_{kr}^{\dagger}\right)\right\|}$$

3.Update the transmit power $\mathbf{p}[\mathbf{t+1}]$, as given (26):

$$p_k[t+1] = \left(\frac{\varsigma_k}{\varphi_k\left(\mathbf{W}[\mathbf{t+1}], \mathbf{p}[\mathbf{t}]\right)}\right) p_k[t]$$

until *convergence*

So, optimization is solved by searching for suitable threshold T_n^{opt}, which the optimal transmit power $\mathbf{p}^{opt}$ has at least one active power constraint. Hence produce same optimal beamforming $\mathbf{W}^{opt}$ and channel gain from Ricean factor κ and BS antenna M. The optimal SIR (SIR maximization) is achieved by the coordination among the macrocells, this is done by reducing one of the performance indicators, so that the design criteria can attain certain point on the optimization.

5.1. Interference Coordination

The coordination is facilitated by transmit power control and exerting control over the spatial reuse of resources (frequency), these tackle interference in the directions. The power ratio $p_{rk} = \frac{p_r}{p_k}$ can be controlled between the kth and rth macro BSs to facilitate reuse of resources. First, based on the power control, the optimal power relation is controlled by the BS antenna. By resource reuse, proper allocation of resource can be reserved for each BS transmits power p_k over the total bandwidth B, but the location of the user impacts the frequency reuse scheme. Now, by employing fractional frequency reuse FFR (for simplicity and tractability), the bandwidth is partitioned into orthogonal sub-bands with fixed number of consecutive subcarrier C, the subchannel is given as $\omega = B/C$. The users at cell-center with low inter-cell interference employ full frequency reuse whilst cell-edge users employ partial frequency reuse to avoid interference with neighboring macro BS [36]. We adopt the soft FFR (SFR) based on resource allocation and BS power control for the cell-center and cell edge users (herein we refer to [23,31] for design). The SFR subchannel has ω frequency sub-bands, where integer $\omega \geq 1$ is frequency reuse factor [41], here all the sub-bands area allocated to each macrocell. Then, to reduce the cell-edge interference and enhance the SIR performance, the BSs require power control $p_{rk} = \frac{p_r}{p_k}$ to transmit with higher power to cell-edge users. Thus, the BS transmits more power to edge region users than center region users according to $P_{n,o} = P_n h_{n,o} \|x_o\|^{-\alpha}$, this improves the SIR and reduces interference at the edge boundary.

6. Numerical Results and Discussions

This section presents the numerical results of the analysis, we use simulations to discuss the theoretical study. Ricean factor κ is selected based on Fig.2.

Preprints (www.preprints.org) | NOT PEER-REVIEWED | Posted: 3 May 2018 doi:10.20944/preprints201805.0072.v1

Peer-reviewed version available at Electronics 2018, 7, 79; doi:10.3390/electronics7060079

Table 3. Table of simulation Parameters for the Heterogeneous Network

Parameter	values
Pathloss exponent α	2.7,3.7,5.7
Distance dependent-pathloss (LOS)	$PL_{LOS} = 103.8 + 20.9\log_{10}(R)$
Distance dependent-pathloss (NLOS)	$PL_{NLOS} = 145.4 + 37.5\log_{10}(R)$
shadowing standard deviation	8dB
Ricean factor κ	0,2,5
users K	32
BS antennas M	128
number of macro BSs	1, 4
macro BS transmit power	30 dBm
number of femto BS	5
femto BS transmit power	3dBm
minimum distance to macro BS	0.035 Km
maximum distance to macro BS R	0.3 Km

Now, Fig.3 shows the distribution of the SIR function with the coverage probability for different macro cell user locations. We validate the result with SIR which the user location r_o increases with lower performance. Thus coverage probability $\mathbb{P}_{\{cov\}}(r_o)$ increases and converge for all user locations r_o at high SIR T_n, confirming that as micro cell users move towards the femto cells in open access system, the received signal is error-prone. But since the low powered BSs are placed almost everywhere within the finite range, the SNR is improved at any distance r_o. The convergence suggest the user is at the cell center, where the femtocell interference is dominate. But, macrocell interference is also dominant at the cell edge. Then probability of coverage always converges at cell edge. Thus macrocell QOS requirement is satisfied at distance $\geq r_o$, or else the user is within femtocell coverage.

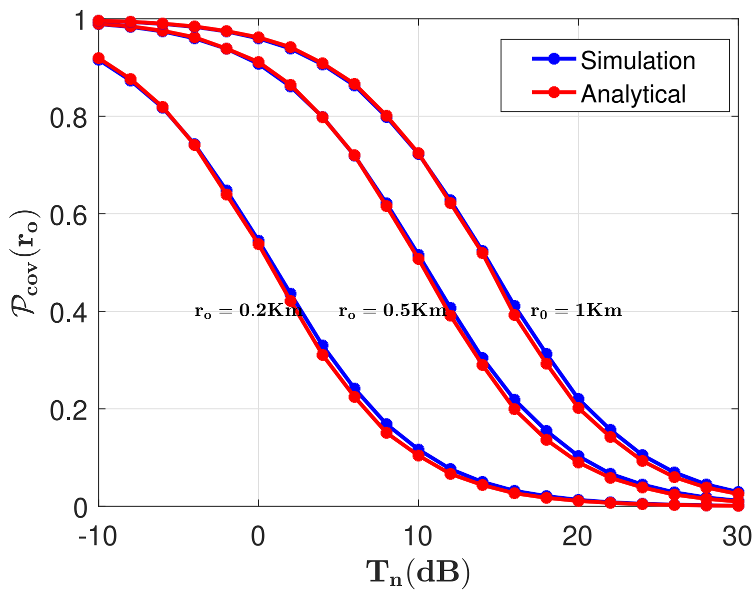

Figure 3. Probability of Coverage as function of quality of service with ($\kappa = 2$)

And, Fig.4 shows the distribution of the SIR function with the coverage probability for different values of the pathloss exponent α. We validate the result with SIR which the pathloss factor α increases with weaken signals thus coverage probability $\mathbb{P}_{\{cov\}}(r_o)$ decreases, and coincide for all pathloss exponents α. Indicating that the network is interference limited as discussed in the analysis. The performance with lower pathloss exponents suggest the coverage is distributed and users are associated with the BSs at closer distance, thus the coverage probability converge at cell edge

Preprints (www.preprints.org) | NOT PEER-REVIEWED | Posted: 3 May 2018 doi:10.20944/preprints201805.0072.v1
Peer-reviewed version available at Electronics 2018, 7, 79; doi:10.3390/electronics7060079

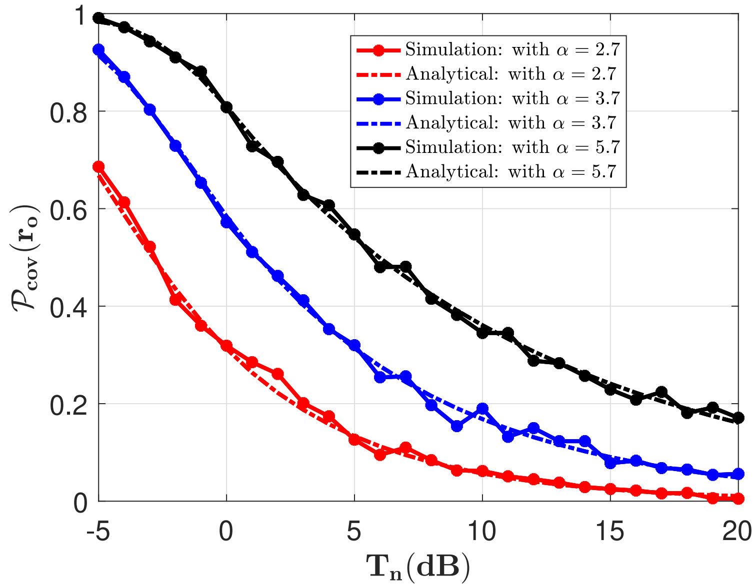

Figure 4. Plot Probaility of coverage versus the SIR comparing performance of different pathoss values with $(\kappa = 2)$

Then, Fig.5 plots the outage probability with the SIR and compares the Ricean factors. Based on the assumption that interference is scattered signals, the Ricean channel with dominant LOS κ has at least one eigenvalue that pre-dominates, thus the MIMO channel behaves as a SISO channel for the largest eigenvalue in achieving the necessary SIR. In addition, from (20) the monotonic increase in κ improves the SIR of a user located within macrocell coverage. But since $\kappa = 0$ has same behavior as scattered signal from femtocell hence the low SIR performance. This suggest that the user is in outage at a location outside the disk radius r_o, if there is no strong macro BS signal.

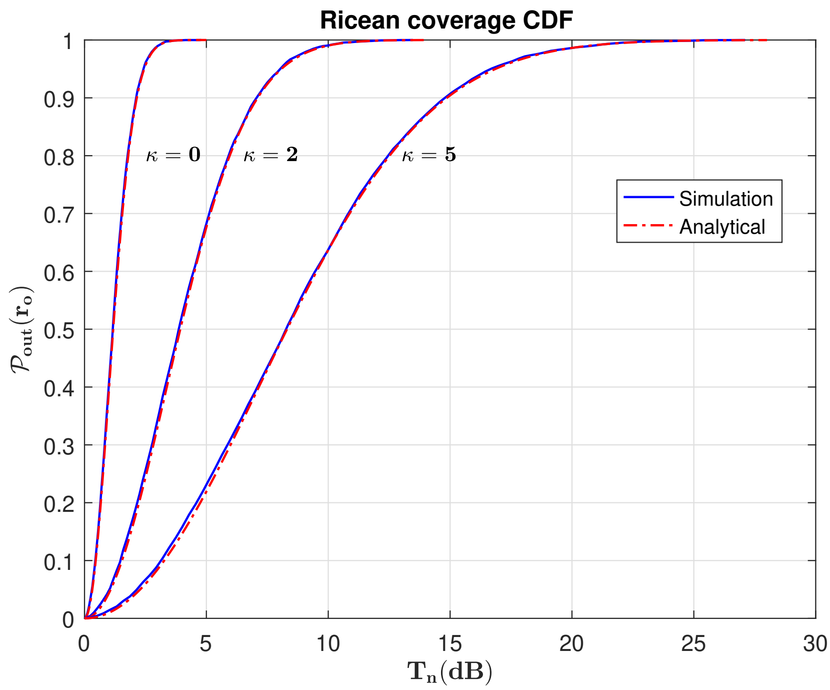

Figure 5. Plotting Outage Probability versus the SIR comparing performance of different Ricean values

Preprints (www.preprints.org) | NOT PEER-REVIEWED | Posted: 3 May 2018 doi:10.20944/preprints201805.0072.v1

Peer-reviewed version available at *Electronics* **2018**, *7*, 79; doi:10.3390/electronics7060079

Also, Fig.6 presents the distribution of the SIR function with the outage probability, here we assume the system is fully loaded , that BSs transmit at maximum power. The Rate parameters in the figure is derived from Shannon instantaneous rate, which takes the form: $[\log_2(1+\varphi_o(r_o)) \leq \text{Rate}] = \{1,2,5,7\}$, where $\varphi_o(r_o) \geq T_n$. From the figure, we can always get average throughput by 5dB in SNR. Note that since the neighboring BSs i.e macro and femto BSs are assigned different instantaneous effective channel distributions, interference is minimized when the user is within macrocell. This helps to improve the instantaneous SIR $\varphi_o(r_o)$, hence the ergodic channel rates. We also observe that the impact of massive MIMO fading channel with $\kappa = 2$ is non-negligible, as such the randomness of the channel affects the SIR, the evidence is seen from the analytical and simulation results. The pre-dominated LOS in the Ricean channel has at least one eigenvalue which corresponds to the MIMO channel behaving like SISO channel, where the largest eigenvalue achieves the maximum gain.

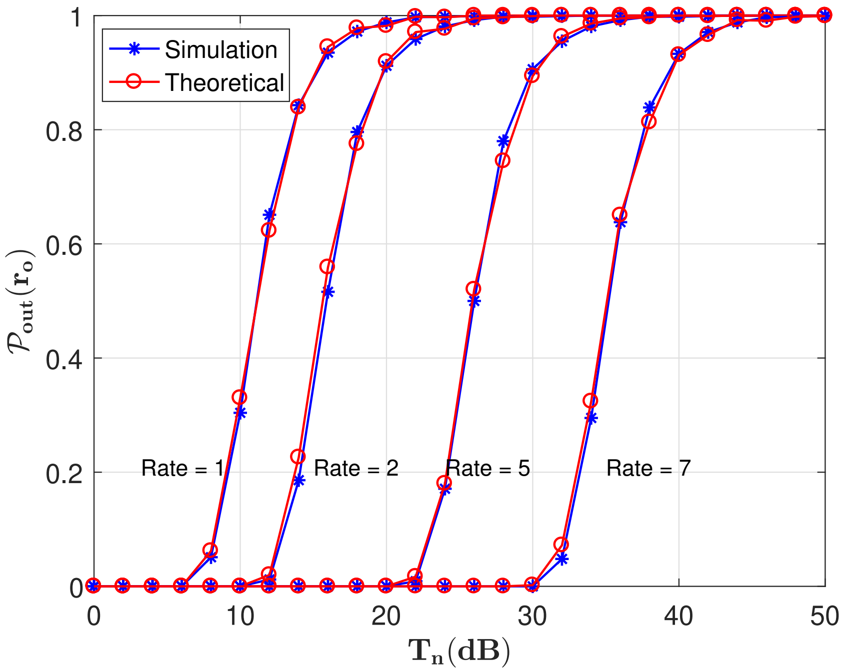

Figure 6. Outage Probability with Quality of service (QOS) target for various cases of Rates

Next, Fig.7 shows the iteration results for the beamforming coordination. The simulation results compare the solver, optimal and non-optimal results. The solver sum rate result is solved by searching for the optimal point, this is done with second-order cone programming (SOCP) problem and solved with the CVX. Furthermore, a search is done to achieve the optimal solution for (25) and produce the required QOS target T_n^{opt} in (28).

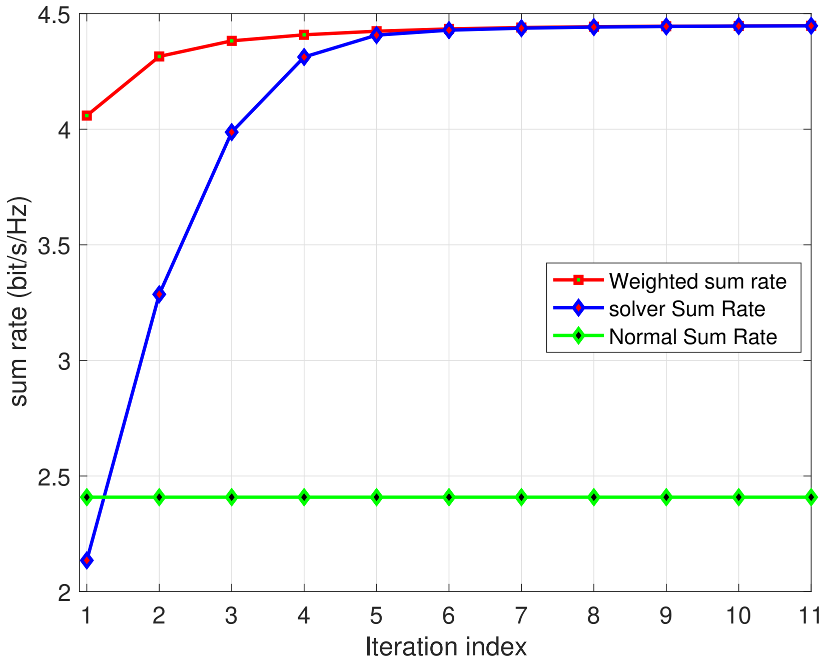

Figure 7. Iteration for the power optimization

Then, Fig.8 presents the Area Spectral Efficiency with number of BS antenna installed to achieve the targeted quality of service. It can be observed in the plot that for smaller number of BS antennas, i.e below 30 antennas, macro BS cooperation is not required as the non-optimal beamforming achieved high QOS target than the optimal beamforming. In practice, small number of transmitting antennas can ensure QOS within a cell, thus the signal strength is not enough to generate more interference. In contrast, for large BS antenna, the optimal Beamform outperform the non-optimal beamforming to achieve the target QOS. This indicates that the optimal beamforming produced a solution to coordinate with other macrocells to achieve the same target. The gap difference enables the macrocell BSs beamforming to improve the ASE without any lost to the max-min optimality.

Peer-reviewed version available at *Electronics* **2018**, *7*, 79; doi:10.3390/electronics7060079

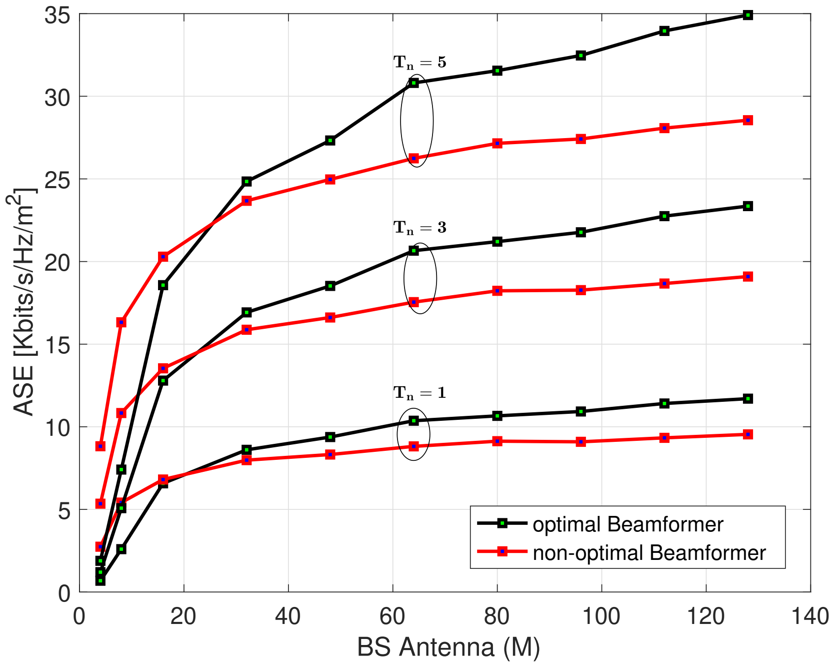

Figure 8. Plot of the Area Spectral Efficiency (ASE) with BS antenna comparing cases of QOS targets

In Fig.9, Compare the Area Spectral efficiency (ASE), BS antenna and Ricean factor. The figure depicts the optimal macro BS and the strength of the LOS component that can guarantee a rate-fairness between the cooperating macrocells. We observe that the max-min optimal beamforming vectors require at least 40 BS antennas and Ricean factor $\kappa = 6$ to achieve ASE and avoid strong channel correlation among macro BSs. Thus with beamform $\mathbf{W}$, the optimal $\mathbf{W}^{opt}$ will use 40 M antennas and $\kappa = 6$ but achieve same rate.

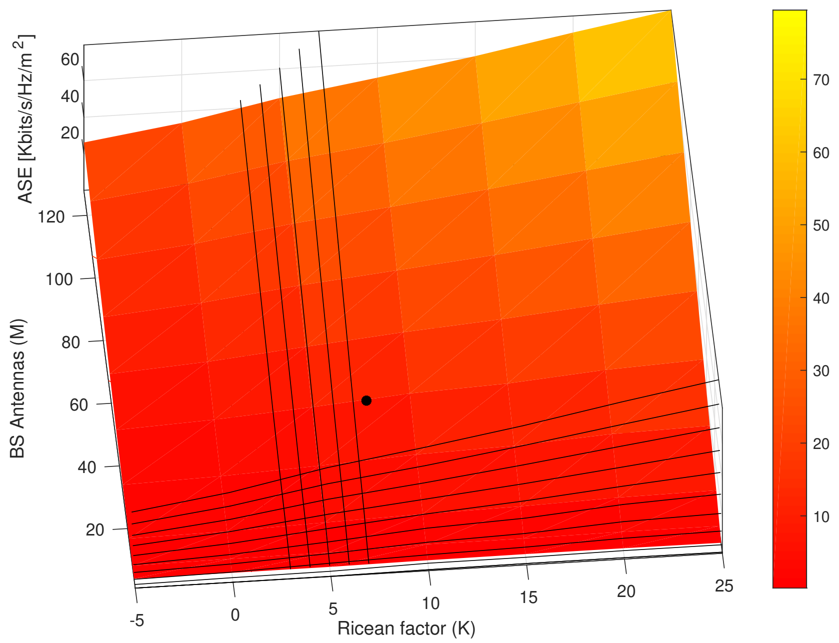

Figure 9. Plot of the ASE with the BS antennas and the Ricean factors

Preprints (www.preprints.org) | NOT PEER-REVIEWED | Posted: 3 May 2018 doi:10.20944/preprints201805.0072.v1

Peer-reviewed version available at *Electronics* **2018**, *7*, 79; doi:10.3390/electronics7060079

The Area Spectral Efficiency, transmit power and Ricean factor is presented in figure 10. Since transmit beamforming enable the transmit power to send the information, the optimal transmit power $\mathbf{p}^{opt}$ in $\mathbf{W}^{opt}$ will require less power than $\mathbf{p}$ in $\mathbf{W}$ but achieve same ASE. This means the served macro BS uses full power whilst other macro BSs use less transmit power. Similarly the optimal Ricean factor $\kappa = 7$ will avoid strong channel correlation in beamforming signal among the macrocells.

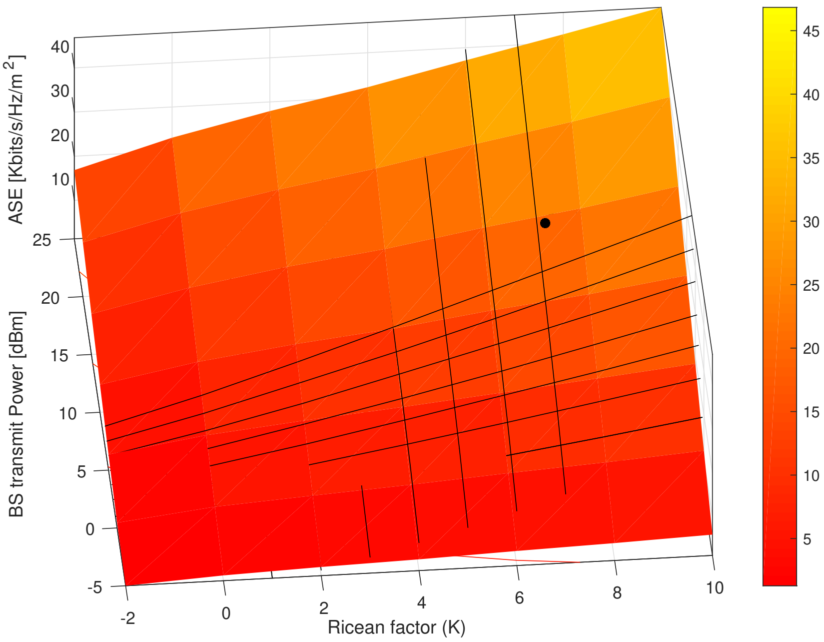

Figure 10. Performance of the ASE versus BS power and Ricean factor

Finally, we compare the probability of outage with the SNR p_k/σ^2 for various cases of quality of service (QOS) in Fig.11. Based on the optimization problem (25), a lower QOS value means the small β_k factor and lower power p_k ensures a low SIR φ_k. Thus the user is located at the cell-edge of the macro cell and prone to outage. In contrast, the higher QOS values corresponds to large β_k factor and high power, with the user located at the cell center. And, since all the QOS cases almost approach convergence it indicates cell-edge effect. Also with low power at macro BS, the BS power can serve more cell-center users than cell-edge which is practically consistent.

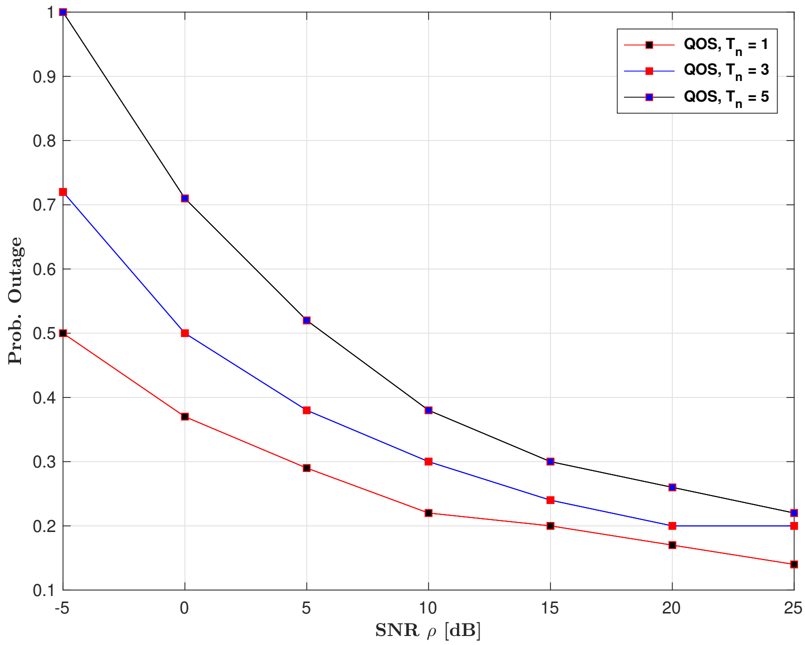

Figure 11. Plot Probability of outage with the SNR, comparing QOS cases.

7. Conclusion

This work considers the stochastic geometry model for the geographical locations of all the BSs and users, and analyze the performance of massive MIMO HetNet. Two multi-path fading are considered, that is Ricean fading for the desired propagation and Rayleigh fading for the interfering propagation. We provide a tractable expression of the typical user SIR for evaluating, probability of coverage, outage Probability and area spectral efficiency (ASE). Based on the derive expressions, simulation results show that the probability of coverage and outage probability converge for different user locations, Ricean factor and pathloss. And, with efficient transmit beamforming coordination, we improve on the ASE performance. The massive MIMO beamforming coordination among the macro BSs through power control, this improves the ASE performance especially at the cell-edge. Then, the optimal BS antennas and Ricean factor provide the level to avoid strong channel correlation in the BS antenna beamforming. The contributions in the work can assist in the discussions and implementation of massive MIMO HetNet for the future network design.

Author Contributions: The authors contributed equally in the paper. This work was was done by J.K.N.N and C.A.M checked and corrected the theoretical and simulation results.

conflict of interest:

The authors declare no conflict of interest.

References

1. Heath, R. W.,Jr; Kountouris,M.; Bai,T. Modeling Heterogeneous Network Interference Using Poisson Point Process. *IEEE Transactions on Signal Processing* **2013**, *61*, 4114 - 4126.
2. ElSawy,H.; Hossain,E.; Haenggi,M. Stochastic Geometric for Modeling, Analysis, and Design of Multi-Tier and Cognitive Cellular Wireless Networks: A Survey. *IEEE Communications Surveys and Tutorials* **2013**, *15*, 996 - 1019.
3. Jo, H. S.; Sang,Y.J.; Xia,P.; Andrews,J.G. Heterogeneous Cellular Networks with Flexible Cells Association: A Comprehensive Downlink SINR Anslysis. *IEEE Transactions on Wireless Communications* **2012**, *11*,3484 - 3494.

4. Yao,R.; Liu,Y.; Lu,L.; Li,G.Y.; Maaref,A. Cooperative Precoding for Cognitive Transmission in Two-Tier Networks. *IEEE Transactions on Communications* **2016**, *64*,1423 - 1436.
5. Wildemeersch,M. Statistical Modeling and Analysis of Interference in Wireless Networks. *University of Twente* **2013**.
6. Baccelli,F.; Blaszczyszyn, B. Stochastic Geometry and Wireless Networks: Volume I Theory. In *Stochastic Geometry and Wireless Networks: Volume I Theory*; Inria-00403039v1; NOW Publishers: Paris,France, 2009.
7. Sanchez-Gracia,J.; Smith,D.R. Capture Probability in Rician Fading Channels With Power Control Transmitter. *IEEE Transactions on Communications* **2002**, *50*,1889 - 1891.
8. Tulino,A.M.; Smith, D.R. Random Matrix Theory and Wireless Communications. In *Foundations and Trends in Communication and Information Theory*,Now Publishers Inc, 2004.
9. Kountouris,.M.; Pappas,N. HetNets and Massive MIMO:Modeling, Potential Gains and Performance Analysis. In *IEEE - APS Tropical Conference on Antennas and Propagation in Wireless Communications* **2013**.
10. Bai,T.;Heath, R. W.,Jr. Analyzing Uplink and Rate in Massive MMO Systems Using Stochastic Geometry. *IEEE Transactions on Communications* **2016**, *64*,4592 - 4606.
11. Li, C.; Zhang,J.; Andrews,J.G.; Letaief,B.K; User-Centric Intercell Interference Nulling for Downlink Small Cell Network. *IEEE Transactions on Communications* **2015**, *63*,1419 - 1431.
12. Li, C.; Zhang,J.; Andrews,J.G.; Letaief,B.K; Success Probability and Area Spectral Efficiency in Multiuser MIMO HetNet. *IEEE Transactions on Communications* **2016**, *64*,1544 - 1556.
13. Tepedelenlioglu, C.; Rajan, A.; Zhang, Y. Applications of Stochastic Ordering to Wireless Communications. *IEEE Transactions on Wireless Communications* **2011**, *10*,4249 - 4257.
14. Haenggi, M. A Geometric Interpretation of Fading in Wireless Networks: Theory and Applications. *IEEE Transactions on Information Theory* **2008**, *54*, 5500 - 5510.
15. Bai,T.;Heath, R. W.,Jr. Location-Specific Coverage in Heterogeneous Networks. *IEEE Signal Processing Letters* **2013**, *20*, 873 - 876.
16. Hosseini ,K.; Yu,W.; Adve,R.S. A Stochastic Analysis of Network MIMO Systems. *IEEE Transactions on Signal Processing* **2016**, *64*,4113 - 4126.
17. Björnson ,E.; Sanguinetti,L.; Kountouris,M. Deploying Dense Networks for Maximal Energy Efficiency: Small Cells Meet Massive MIMO. *IEEE Journal on Selected Areas in Communications* **2016**, *34*,832 - 847.
18. Weber,S.; Andrews,J.G.; Jindal,N. An Overview of the Transmission Capacity of Wireless Networks. *IEEE Transactions on Communications* **2010**, *58*,3593 - 3604.
19. Renzo,M.D; Guidotti ,A; Corazza ,G.E. Average Rate of Downlink Heterogeneous Cellular Networks over Generalized fading Channels: A Stochastic Geometry Approach. *IEEE Transactions on Communications* **2013**, *61*,3050 - 3071.
20. Ding, M.; Wang, P.; Lopez-Perez D.;Mao G.;Lin, Z. Performance Impact of LOS and NLOS Transmissions in Dense Cellular Networks. *IEEE Transactions on Wireless Communications* **2016**, *15*,2365 - 2380.
21. Yang,X.; Fapojuwo, A.O. Coverage Probability Analysis of Heterogeneous Cellular Networks in Rician/Rayleigh Fading Environments. *IEEE Communications Letters* **2015**, *19*,1197 - 1200.
22. Srinivasa, S.;Haenggi, M. Distance Distributions in finite Uniformly Random Networks: Theory and Applications. *IEEE Transactions on Vehicular Technology* **2010**, *59*, 940 - 949.
23. Zhuang,H.;Ohtsuki,T. A Model Based on Poisson Point Process for Analyzing MIMO Heterogeneous Networks Utilizing Fractional Frequency Reuse. *IEEE Transactions on Wireless Communications* **2014**, *13*,6839 - 6850.
24. Andrews,J.G.; Baccelli,F.; Ganti,R.K. A Tractable Approach to Coverage and Rate in Cellular Networks. *IEEE Transactions on Communications* **2011**, *59*,3122 - 3134.
25. Peng,M.;Li,Y.;Quek, T.Q.S.;Wang, C. Device-to-Device Underlaid Cellular Networks Under Rician Fading Channels. *IEEE Transactions on Wireless Communications* **2014**, *13*, 4247 - 4259.
26. Li, Y.; Li,J.;Peng, M. Performance Analysis of Device-to-Device Underlay Communication in Rician Fading Channels. In *IEEE - GLOBECOM 2013* **2013**.
27. Wang, L.C.;Liu, W.C.;Cheng, Y.H. Statistical Analysis of a Mobile-to-Mobile Rician Fading Channel Model. *IEEE Transactions on Vehicular Technology* **2009**, *58*, 32 - 38.
28. Karipidis,E.; Sidiropoulos,N.D.; Luo,Z.Q. Quality of Service and Max-Min Fair Transmit Beamforming to Multiple Co-channel Multicast Groups. *IEEE Transactions on Signal Processing* **2008**, *56*,1268 - 1278.

29. Nguyen, D.H.N;Le, L.B.;le Ngoc, T. Multiuser Admission Control and beamforming Optimization Algorithms for MISO Heterogeneous Networks. *IEEE Access* **2015**, *3*.
30. Dhillon, S.H.;Ganti, K.R.;Baccelli, F.;Andrews J.G. Modeling and Analysis of K-Tier Downlink Heterogeneous Cellular Networks. *IEEE Journal on Selected Areas in Communications* **2012**, *30*, 550 - 560.
31. Davaslioglu,K.; Coskun,C.C.; Anyanoglu,E. Energy-Efficient Resource Allocation for Fractional Frequency Reuse in Heterogeneous Networks. *IEEE Transactions on Communications* **2015**, *14*,5484 - 5497.
32. Kuhn V.:Wireless Communications Over MIMO Channels: Applications to CDMA and Multiple Antenna Systems. John Wiley & Press (2006)
33. Tse D.,Viswanath P.:Fundamentals of Wireless Communication. Cambridge University Press (2005)
34. Vergara ,V.M.; Barbin,S.E. LOS and NLOS Components in MIMO Rice Fading Channels. In *IEICE - Proceedings of Asia - Pacific Conference* **2010**.
35. Gradshteyn,I.S.; Ryzhik, I.M. Integrals and Series. In *Table of Integrals, Series, and Products*; Jeffrey,A., Zwillinger, D.,7th.; Elsevier Academic Press: London, UK, 2009.
36. Mahmud,A.; Hamdi,K.A. A Unified Framework for the Analysis of Fractional Frequency Reuse Techniques. *IEEE Transactions on Communications* **2014**, *62*,3692 - 3705.
37. Jeong,Y.; Quek,T.Q.S. Beamforming Optimization for Multiuser Two-Tier Networks. *Journal of Communications and Networks* **2011**, *13*, 327 - 338.
38. Boyed S. and Vandenerghe L.: Convex Optimization. Cambridge Uni. Press (2004)
39. Goldsmith, A. Statistical Multipath Channel Models. In *Wireless Communications*; Cambridge University Press, 2005.
40. Matskani,E.; Sidiropoulos, N.D.;Luo, Z.Q.;Tassiulas, L. Convex Approximation Techniques for Joint Multiuser Downlink Beamforming and Admission Control. *IEEE Transactions on Wireless Communications* **2008**, *7*,2682 - 2693.
41. Atzen,A.; Arnau,J.; Debbah,M. Fractional Pilot Reuse in Massive MIMO Systems. In *IEEE International conference on Communication Workshop (ICCW)* **2015**, *Series: DOI:10.1109/1CCW.2015.7247312*.